Storage-less and converter-less maximum power point tracking of photovoltaic cells for a nonvolatile microprocessor

Cong Wang*, Naehyuck Chang†, Younghyun Kim†, Sangyoung Park†,
Yongpan Liu*, Hyung Gyu Lee‡, Rong Luo* and Huazhong Yang*

Tsinghua National Laboratory for Information Science and Technology, Tsinghua University, China*
Department of EECS/CSE, Seoul National University, Korea†
School of Computer and Communication Engineering, Daegu University, Korea‡
ypliu@tsinghua.edu.cn*, naehyuck@elpl.snu.ac.kr†, hgichon2@hotmail.com‡

***Abstract*—This paper pioneers the maximum power point tracking (MPPT) of photovoltaic (PV) cells that directly supply power to a microprocessor without an energy storage element (a battery or a large-size capacitor) nor power converters. The maximum power point tracking is conventionally performed by an MPPT charger that stores in the energy storage element, and a voltage regulator (typically a DC-DC converter) produces a proper voltage level for the microprocessor. The energy storage element is an energy buffer and makes it possible to perform MPPT of the PV cells and power management of the microprocessor independently. However, the energy storage element, MPPT charger and DC-DC converter cause seriously limited lifetime (when a typical battery is adopted), significant energy loss (typically over 20%), increased weight/volume and high cost, etc. The proposed method enables extremely fine-grain dynamic power management (DPM) in every a few hundred microseconds and performs the MPPT without using an MPPT charger and a DC-DC converter as well as an energy storage element. We achieve 84.5% of energy harvesting efficiency using the proposed setup with huge reduction in cost, weight and volume, and extended lifetime, which is not even numerically comparable with conventional MPPT methods.**

I. Introduction

Energy harvesting gives a potential to make an electronics system sustainable and maintenance free. Any form of energy such as kinetic, thermal, etc., can be transformed to electrical energy, and photovoltaic (PV) cell is one of the most practical energy harvesting for electronics circuits in terms of power capacity, voltage and current magnitudes, cost, volume, weight, and so forth.

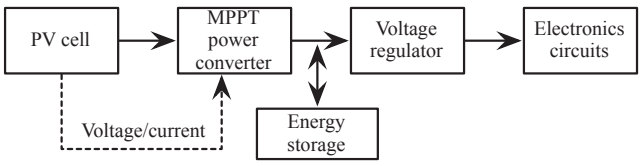

Fig. 1. Typical architecture of a solar energy harvesting system with MPPT.

Fig. 1 shows a typical architecture of a solar energy harvesting system with the maximum power point tracking (MPPT) [1] or maximum power transfer tracking (MPTT) [2]. A PV module requires MPPT because its internal impedance is not low enough to be a voltage source like conventional batteries. Furthermore, the MPP largely varies with the solar irradiance and temperature, which requires continuous tracking of the MPP. Common MPPT continuously maintains the MPP by the use of a perturb-and-observe method [3]. The MPP current can hardly match with the power supply current of the electronics. Power supply current of a microprocessor continuously fluctuates. In other words, the PV energy harvesting system will generally fail MPPT if the electronics is directly connected to the PV cell without an energy buffer. The PV cell output voltage largely fluctuates as the microprocessor power supply current changes, which makes the PV cell output voltage change. In addition, the terminal voltage of typical energy storage devices generally does not match with the supply voltage of microprocessors. For example, Li-ion battery single cell voltage is commonly 3.7 V. The above reasons make a PV energy harvesting system to equip with two cascaded power converters (an MPPT charger and a DC-DC converter) and energy storage device, a battery or equivalent, in the middle. Such a setup has been widely used undoubtedly.

This work was supported in part by the NSFC under grant 61271269, High-Tech Research and Development (863) Program under contract 2013AA01320, the Importation and Development of High-Caliber Talents Project of Beijing Municipal Institutions under contract YETP0102, the Center for Integrated Smart Sensors funded by the Ministry of Science, ICT & Future Planning as Global Frontier Project (CISS-201373718) and the NRF of Korea funded by the MEST (No. 2013035079). The ICT at Seoul National University provides research facilities for this study. Jaehyun Park of Seoul National University assisted with the evaluation board development.

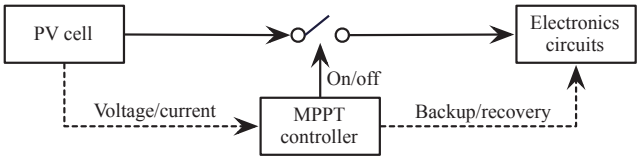

Fig. 2. Proposed converter-less and storage-less energy harvesting system architecture with MPPT.

However, there are serious disadvantages from the power converters and the energy storage device though they were mandatory to make a PV energy harvesting system functional. First, the power converters and energy storage devices are typically the most expensive, heaviest, and largest components in a PV energy harvesting system. It is difficult and costly to integrate the expensive and bulky passive components, such as bulk capacitors, multilayer ceramic capacitors, inductors, etc. on chip. Second, the energy storage device, typically a rechargeable battery, is the primary component that significantly shortens the system lifetime or requires periodic maintenance of the system. These two factors seriously discourage the deployment of small, low-cost and self-sustainable ubiquitous smart sensors in various applications.

Elimination of the power converter and energy storage device gives a great freedom in size, cost, volume, lifetime, and you name it. However, there are obvious obstacles in such a radical approach. First, the MPP current and voltage should be exactly matched with the electronics supply voltage and current. Typical microprocessors cannot fulfill this requirement in general. Second, the electronics should be functional even after power interrupt when the solar irradiance is not strong enough to operate the electronics.

In this paper, we propose a converter-less and storage-less energy harvesting system that performs the MPPT. To the best of knowledge, this is the first paper that attempts storage-less and converter-less MPPT. We overcome the above mentioned obvious obstacles by the use of i) PV cell V-I characteristics and ii) a nonvolatile microprocessor. The PV cell MPP voltage is maintained within a narrow range regardless of the solar irradiance. In other words, the PV

978-1-4799-2816-3/14/$31.00 ©2014 IEEE

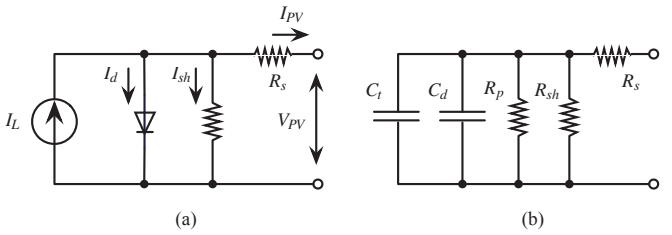

Fig. 3. (a) A DC equivalent circuit of a PV module; (b) An AC equivalent circuit of a PV module.

cell produces an almost-constant voltage output as long as we keep track of the MPP current. The nonvolatile microprocessor provides extremely fast context saving and restoration before and after power interrupt, which makes a very fine-grain dynamic power management (DPM) feasible. Fast enough DPM makes the PV cell keep the MPP as if the electronics load current is a DC current as long as the average current is the same as the MPP current.

There are huge advantages from the proposed method as long as the target applications fit to the design philosophy. The advantages in terms of lifetime, cost, volume, weight, etc., are not even numerically comparable with conventional energy harvesting systems. The proposed method is not operational after sunset. However, the proposed PV energy harvesting systems are functional even with a very weak solar irradiance thanks to a very fine-grain DPM in a few hundred microseconds, which make a ultra low duty operation possible.

Experiment results show that the proposed storage-less and converter-less PV energy harvesting system with MPPT mitigates the high energy loss stemmed from power converters and state transitions, achieving an overall system efficiency of 84.5%. The proposed system executes $40\% - 2.5X$ more tasks than conventional baseline systems given the same PV cells and solar irradiance in a day.

II. Component Models

A. Photovoltaic Module

We use a well-known single diode equivalent circuit model to describe the DC characteristics of a PV module as shown in Fig. 3. The I-V characteristic of a PV module is represented by (1) and (2) [4].

$$I_{pv} = I_L - I_0(e^{\frac{V_{pv}+I_{pv}R_s}{a}} - 1) - \frac{V_{pv}+I_{pv}R_s}{R_{sh}}, \tag{1}$$

$$a \equiv \frac{N_s n_1 k T_c}{q}, \tag{2}$$

where N_s, n_1, k, T_c and q indicate the number of cells in series, the ideality factor of the diode, the Boltzmann's constant, the module temperature, and the electron charge, respectively.

We extract the five parameters (I_L, I_0, n_1, R_s, R_{sh}) with a curve-fitting method. We first measure a set of voltage-current points under a reference condition (solar irradiance of 200 W/m^2 and temperature of 27 $^\circ C$), and then obtain the best-fit parameters that minimize the deviation between the curve provided by the model and the measured points. These parameter values are only valid for the reference condition. We use (3), (4) and (5) introduced in [5] to obtain PV characteristics at other temperature and solar irradiance conditions.

$$I_L = \frac{S}{S_{ref}}\left[I_{L,ref} + \alpha_{I_{sc}}(T_c - T_{c,ref})\right], \tag{3}$$

$$\frac{I_0}{I_{0,ref}} = \frac{T_c}{T_{c,ref}} \exp\left[\frac{E_g}{k}\left(\frac{1}{T_c} - \frac{1}{T_{c,ref}}\right)\right], \tag{4}$$

$$\frac{R_{sh}}{R_{sh,ref}} = \frac{S_{ref}}{S}, \tag{5}$$

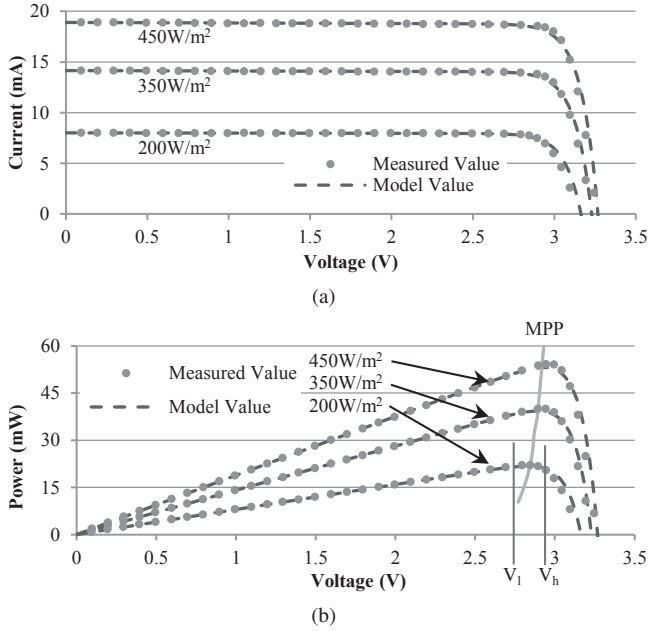

Fig. 4. (a) I-V curve; (b) P-V curve of a 4.5×5.5 cm^2 experimental photovoltaic module under different solar insolation at the temperature of 300K. An MPPT window is shown on the curve for the irradiance of $200W/m^2$.

where S and E_g indicate the solar irradiance in W/m^2, and the material band gap energy, respectively. Symbols with subscript $[*]_{ref}$ are values under the reference condition. Following the investigation in [4], we assume the series resistance R_s and diode ideality factor n_1 are independent of temperature and solar irradiance in this paper.

TABLE I
Model Parameters of the Experimental PV Module
(Test Condition: $S = 200W/m^2$, $T_c = 300K$).

I_L	I_0	n_1	R_s	R_{sh}	N_s
$8.01mA$	$1.01^{-16}A$	1.885	0.17Ω	$22.36k\Omega$	2

Table I lists the five parameters of a PV module extracted from measurement results. As illustrated in Fig. 4(a), the model value fits well with the actual characteristic of the PV module.

The MPPT technique is widely used in PV systems. The MPP voltage is relatively stable regardless of the solar irradiance as shown in Fig. 4(b). We emphasize that the PV module output voltage variation is small enough even with different solar irradiance levels as long as we track the MPP. It is possible to remove the DC-DC converter between the PV module and the load device if the MPP voltage is also within the operating range of the load device. In other words, tracking the MPP implies output voltage regulation of the PV module.

B. DC-DC Converter

DC-DC converters convert and regulate the input voltage to a desired output voltage. Switching-mode DC-DC converters are generally used for voltage regulation as they are known to be more power efficient than linear voltage regulators [6, 7]. The efficiency of a switching DC-DC converter is defined as follows.

$$\eta_{conv} = \frac{P_{out}}{P_{in}} = 1 - \frac{P_{conv}}{P_{in}}, \tag{6}$$

where P_{in}, P_{out} and P_{conv} are input power, output power, and power loss in the converter, respectively.

The converter efficiency typically ranges from 10% to 80% due to the conduction power dissipation, gate drive power dissipation

and controller power dissipation [8]. Moreover, conventional energy harvesting system is typically equipped with two stages DC-DC converters, as shown in Fig. 5(a). One is the input-stage power converter, which is typically an MPPT converter that charges the energy storage device with the PV module power. The other is a voltage regulator at the output stage. This two-stage converter system significantly degrades the power efficiency of the whole PV energy harvesting system. It would give a great potential to achieve tremendous power efficiency enhancement if we remove the power converters from a PV energy harvesting system.

C. Nonvolatile Processor

A nonvolatile processor is highly desired in a very frequent DPM because of its extremely low overheads in system states backup and recovery [9]. A recent work fabricated a nonvolatile microprocessor named THU1010N using a 130 *nm* ferroelectric technology from Rohm, where nonvolatile elements are incorporated into each conventional volatile flip-flop [10]. Data movement between flip-flops and their local nonvolatile elements are performed in parallel, thus expediting the backup and recovery processes.

TABLE II
SPECIFICATIONS OF THE NONVOLATILE MICROPROCESSOR USED IN EVALUATION PROTOTYPE.

Component	Part No.	Voltage Range	Power Consumption	Transition Overhead	
				Backup	Recovery
NVCPU	THU1010N	2.7 V – 3.6 V	5.78 mW	8 μs	3 μs

Table II summarizes the power consumption and transition overheads of the THU1010N nonvolatile microprocessor that we use in the proposed storage-less and converter-less PV energy harvesting system with MPPT. The backup and recovery time of the nonvolatile microprocessor are only 8 μs and 3 μs, respectively, being three to four orders of magnitude faster than typical microprocessors.

III. STORAGE-LESS AND CONVERTER-LESS MPPT

A. System Architecture

Fig. 5(a) illustrates the architecture of conventional solar energy harvesting system, which is in a typical two-tier setup. The MPPT charger maintains the PV operation at the MPP, extracting as much power as possible from the PV module, and stores it in the energy storage device. The harvested energy is retrieved from the storage device and delivered to the load device via power converters.

We mitigate the efficiency loss caused by the DC-DC converters, the degradation of lifetime, weight, volume stemmed from the energy storage unit, and the potential high cost incurred from both of them,

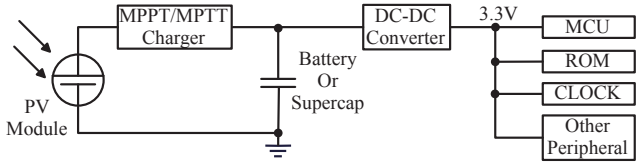

(a) Conventional energy harvesting system.

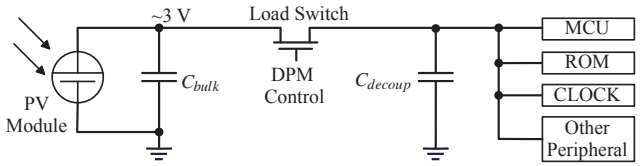

(b) The proposed storage-less and converter-less PV energy harvesting system.

Fig. 5. System diagram of the conventional and proposed architecture.

proposing a novel storage-less and converter-less architecture shown in Fig. 5(b). We connect the PV module to the electronics devices, the nonvolatile microprocessor, an OTP (one-time programming) ROM and peripherals, via a load switch. The MPP tracker (omitted in Fig. 5(b)) continuously turns on and off the load switch. The MPP controller controls the effective duty cycle of the nonvolatile microprocessor. This control process acts like the MPP tracking with the PV module current steering as the load switch turns on and off faster than the cut off frequency of the PV module. We keep the PV module output voltage close to the MPP voltage at all times. We carefully select the PV module that has the MPP voltage close to the legal operating voltage of the semiconductor devices. This makes the PV energy harvesting system operational without power converters nor an energy storage device while performing the MPPT.

There is a bulk capacitor connected in parallel with the PV cell. It extends the time constant of the PV module so that the PV module time constant may match with the feasible DPM period of the nonvolatile microprocessor. There is a decoupling capacitor on the load side, which maintains power integrity of the semiconductor devices.

Table III summarizes the power consumption and transition overheads of the components that we use in the evaluation prototype. The ROM is used as a code storage.

TABLE III
SPECIFICATIONS OF THE COMPONENTS USED IN EVALUATION PROTOTYPE.

Component	Part No.	Power Consumption	Transition Overhead	
			Backup	Recovery
ROM	AT27LV010A	16.50 mW	0	2 μs
Load Switch	TPS27081	0.31 mW	0	250 ns
Clock	74HC14	2.84 mW	0	2 μs
Other Peripheral	LCD and Sensors	14.56 mW	N/A	N/A

B. The MPPT with Fine-Grain Dynamic Power Management

We achieve the MPPT with fine-grain DPM of the nonvolatile microprocessor and associated peripherals. We adjust the average load current, as a result of the DPM, and attempt to match the load equivalent resistance with the internal resistance of the PV module. We turn on the nonvolatile microprocessor and its peripherals when the PV module output voltage is higher than the upper threshold, V_h (see Fig. 4). The PV module output voltage decreases as the load devices are connected to the PV module and the load current is higher than the MPP current. We assume the PV module size is over-designed if the load current is lower than the MPP current. The PV module output voltage becomes lower than the MPP voltage and then even lower than the lower threshold, V_l. The MPP controller switches off, and the PV module voltage recovers and goes back to V_h. This control policy maintains the PV module output voltage within $[V_l, V_h]$. We do not consider expensive dynamic voltage and frequency control in this paper.

A traditional microprocessor saves the data in volatile registers into a nonvolatile memory, for example a discrete FeRAM or Flash, before power-off and restores back to the their original places after power-on. Such context saving and restoration is done serially in conventional systems, and is very slow due to the limited IO bandwidth, resulting in large time and energy overheads. On the other hand, with a nonvolatile microprocessor, system states backup and recovery is no longer the bottleneck when we perform DPM.

IV. PROPERTIES OF STORAGE-LESS AND CONVERTER-LESS MPPT

We assume the load power consumption during the state transition ($P_{on,off}$ for backup and $P_{off,on}$ for recovery) is the same as the power consumption in ON state (P_{on}), i.e., $P_{on} = P_{on,off} = P_{off,on}$. The

MPPT window [V_l, V_h] is narrow enough and the power dissipated in the load switch, P_{sw}, is a constant.

A. Load switch is OFF

The load devices are shut down, and the PV cell charges the bulk capacitor when the load switch is OFF. With the Kirchhoff's current law (KCL), we have

$$I_{pv} = C_{bulk}\frac{\mathrm{d}V_{pv}}{\mathrm{d}t}. \tag{7}$$

We derive the time to recover the bulk capacitor voltage from V_l to V_h as follows.

$$T_{l,h} = T_{off} = \int_{V_l}^{V_h} \frac{C_{bulk}}{I_{pv}}\mathrm{d}V_{pv}, \tag{8}$$

where T_{off} represents how long the load switch and load device are kept in OFF state, and C_{bulk} is the size of the bulk capacitor.

The terminal voltage of the decoupling capacitors quickly drops down to 700 mV in our setup as soon as the load switch is OFF since there is no further power supply from the PV module. We assume the 700 mV is related to the threshold voltage of the transistors in the nonvolatile microprocessor. The terminal voltage continues to drop as time elapses, but it is relatively very slow compared with the DPM period we apply. We regard the terminal voltage of the decoupling capacitors, $V_{C_{decomp}}$ is 700 mV when the load switch is OFF, and we denote it as V_{th}.

B. Load switch is ON

The load switch would be turned ON once the bulk capacitor is charged to V_h.

1) Charge sharing: The charges in the bulk capacitor are shared with the decoupling capacitor C_{decoup} at the output stage immediately after the load switch is ON, resulting in an instant voltage drop of the bulk capacitor (PV cell) from V_h to V_{mid}. The value of V_{mid} is determined according to the law of charge conservation:

$$V_{mid} = \frac{C_{bulk}V_h + C_{decoup}V_{th}}{C_{bulk} + C_{decoup}}. \tag{9}$$

The resistance of the load switch in ON state is generally very low (tens to hundreds of $m\Omega$), and the charge sharing process is almost finished instantly. Therefore, we omit the time that bulk capacitor voltage drops from V_h to V_{mid}.

2) OFF-to-ON transition: The node goes into OFF-to-ON transition after the charge sharing process. The microprocessor restores its states and other components. We denote the OFF-to-ON transition time as $T_{off,on}$.

3) Task execution: Once the OFF-to-ON transition is over, the node goes into normal operation and start executing its tasks. We denote the time that allows the node to execute tasks as T_{task}.

4) ON-to-OFF transition: The voltage of the bulk capacitor drops during the task execution time. The MPP tracker keeps watching the voltage drop. When $V_{C_{bulk}}$ becomes close to V_l, it forces the node to backup its states and prepare to go to OFF mode. We denote the time reserved for system states backup before turning OFF the load switches as $T_{on,off}$.

We assume $P_{on} = P_{on,off} = P_{off,on}$, and during the load switch is ON, with the law of conservation of energy, we have

$$V_{pv}I_{pv} = P_{on} + P_{sw} + (C_{bulk} + C_{decoup})V_{pv}\frac{\mathrm{d}V_{pv}}{\mathrm{d}t}. \tag{10}$$

We obtain the time it takes for PV cell voltage V_{pv} (also the bulk capacitor voltage $V_{C_{bulk}}$) to drop from V_h to V_l, denoted by $T_{h,l}$.

$$T_{h,l} = T_{off,on} + T_{task} + T_{on,off} = \int_{V_{mid}}^{V_l} \frac{(C_{bulk} + C_{decoup})V_{pv}}{V_{pv}I_{pv} - P_{on} - P_{sw}}\mathrm{d}V_{pv}. \tag{11}$$

The integral on the right side starts from V_{mid} and ends with V_l because we ignore the time of the instant charge sharing. The size of the bulk capacitor and the operating voltage region $[V_l, V_h]$ should ensure that $T_{task} > 0$. Otherwise there is no time for actual task execution during time period $T_{h,l}$.

C. Fine-grain DPM Efficiency

We derive the energy efficiency of the proposed system η_{sys} in one DPM cycle with (8) and (11) as well as the transition overhead specifications of the components:

$$\eta_{sys} = \frac{E_{task}}{E_{mpp}} = \frac{P_{on}T_{task}}{P_{mpp}(T_{h,l} + T_{l,h})}, \qquad (P_{mpp} < P_{on}), \tag{12}$$

where E_{task} is the effective energy used for task execution, and E_{mpp} and P_{mpp} are the maximum energy and maximum power that can be extracted from the PV cell, respectively. The load switches are always ON and the extra energy would be wasted if the harvested power exceeds the demand of the load device.

$$\eta_{sys} = \frac{P_{on}}{P_{mpp}}, \qquad (P_{mpp} \geq P_{on}). \tag{13}$$

However, we do not assume this situation in this paper because it is over-designed.

The period of the DPM cycle is defined as

$$T_{dpm} = T_{h,l} + T_{l,h}, \tag{14}$$

where the duty ratio is

$$D_{dpm} = \frac{T_{h,l}}{T_{dpm}}. \tag{15}$$

D. Effects of the Bulk Capacitor

The sizing of bulk capacitor plays an important role because it determines the DPM time granularity, voltage drop during charge sharing, and the time and energy overhead of the DPM scheme. The DPM period can be estimated by (16), assuming that the PV module output power is close to its MPP in voltage range [V_l, V_h].

$$T_{dpm} \approx (\frac{V_h - V_l}{I_{pv,mpp}} + \frac{V_{mid} - V_l}{I_{on} - I_{pv,mpp}})C_{bulk}. \tag{16}$$

So the larger the bulk capacitor size, the longer the DPM period. Furthermore, if the bulk capacitor size is small, the terminal voltage decreases fast as the load current discharges the capacitor, and larger voltage drop occurs during charge sharing. If the bulk capacitor is large, the terminal voltage decreases slowly, and small voltage drop occurs during charge sharing. A larger capacitor makes it harder to track MPP of solar cell and perform finer-grain MPPT, but it lowers energy loss due to charge sharing and state transitions because the DPM is less frequent.

V. Experiments

A. Experimental Setup

We compare the efficiency of the proposed system with two baseline systems. The architecture of the first baseline system, called the *volatile microprocessor baseline*, is shown in Fig. 5(b) assuming the microprocessor is a conventional volatile microprocessor with nonvolatile FRAM backup. The backup and recovery time overheads of this volatile microprocessor are 300 μs and 200 μs, respectively. The second baseline system, called the *conventional MPTT baseline*, is the system illustrated in Fig. 5(a).

The MPP tracking for the proposed system and the volatile microprocessor baseline system are based on the constant voltage principle, where the voltage window $[V_l, V_h]$ is set to be $[2.75\ V, 2.90\ V]$. The bulk capacitor size is 4.7 μF and decoupling capacitor is 20 nF. The conventional MPTT baseline has a 0.2 F supercapacitor as the energy storage device. We adopt the model parameters introduced in [2] for the converters in the conventional MPTT baseline.

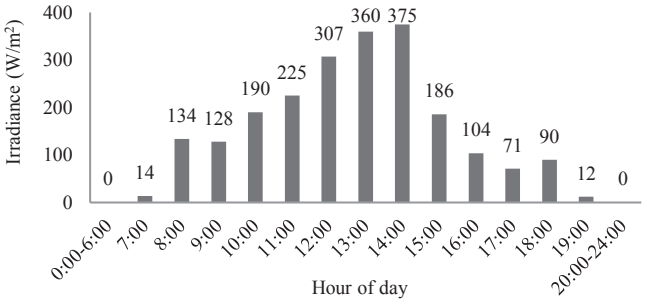

Fig. 6. Hourly solar irradiance during a day.

All the three systems are powered by the same PV module and have the same load power consumption. The PV module size is $4.5 \times 5.5\ cm^2$, with the nominal MPP voltage of 3 V. Model parameters for the PV module and component specifications for the load device are summarized in Table I and III, respectively.

B. System Efficiency

Fig. 6 depicts the hourly solar radiation data on a partly cloudy day that is chosen from the NSRDB (National Solar Radiation Data Base). The irradiance value is the average solar irradiance during the last one hour. We assume the solar irradiance changes every hour for simplicity in calculation, but actual deployment of the proposed method is not restricted by such assumption. The three systems are exposed to the solar irradiance characterized by Fig. 6, and we compare the overall energy efficiency of each system in a whole day.

TABLE IV
DYNAMIC POWER MANAGEMENT RESULTS.

Common DPM statistics					Proposed System			Volatile Microprocessor Baseline		
Time	V_{mpp} (V)	T_{dpm} (μs)	D_{dpm}	E_{mpp} (J)	Work	E_{task} (J)	η_{sys} (%)	Work	E_{task} (J)	η_{sys} (%)
7:00	2.50	N/A	N/A	4.83	No	0	0	No	0	0
8:00	2.73	218	31.6%	50.14	Yes	36.38	72.6	No	0	0
9:00	2.72	224	30.0%	47.81	Yes	34.30	71.7	No	0	0
10:00	2.76	191	46.9%	71.95	Yes	57.07	79.3	No	0	0
11:00	2.78	195	56.5%	85.69	Yes	71.25	83.1	No	0	0
12:00	2.80	301	79.7%	118.14	Yes	108.37	91.7	No	0	0
13:00	2.82	1100	95.1%	139.27	Yes	135.39	97.2	Yes	65.74	47.2
14:00	2.82	1360	99.6%	145.27	Yes	143.72	98.9	Yes	138.34	95.2
15:00	2.76	192	45.8%	70.38	Yes	55.51	78.9	No	0	0
16:00	2.70	260	23.6%	38.57	Yes	26.27	68.1	No	0	0
17:00	2.67	369	14.8%	25.98	Yes	15.90	61.2	No	0	0
18:00	2.69	294	19.9%	33.21	Yes	21.78	65.6	No	0	0
19:00	2.50	N/A	N/A	4.11	No	0	0	No	0	0
Overall				835.34		705.94	84.5		204.08	24.4

Table IV shows the simulation results for the proposed system and the volatile microprocessor baseline. The PV energy harvesting system is not continuously operational with the duty ratio less than 100% from 7:00 to 18:00 because the PV module we use is not overly large. The DPM period are mostly around $200-400\ \mu s$, except being over 1 *ms* during 12:00–14:00. The proposed system works in most of the time thanks to the low transition overhead of the nonvolatile microprocessor, achieving an overall system efficiency of 84.5%. On the other hand, the traditional volatile microprocessor suffers from its large transition overhead. The volatile microprocessor baseline only works during 12:00-14:00 because only during this period the load switch ON duration is longer than its transition overhead, providing time for task execution. The overall efficiency of the volatile microprocessor baseline is only 24.4%.

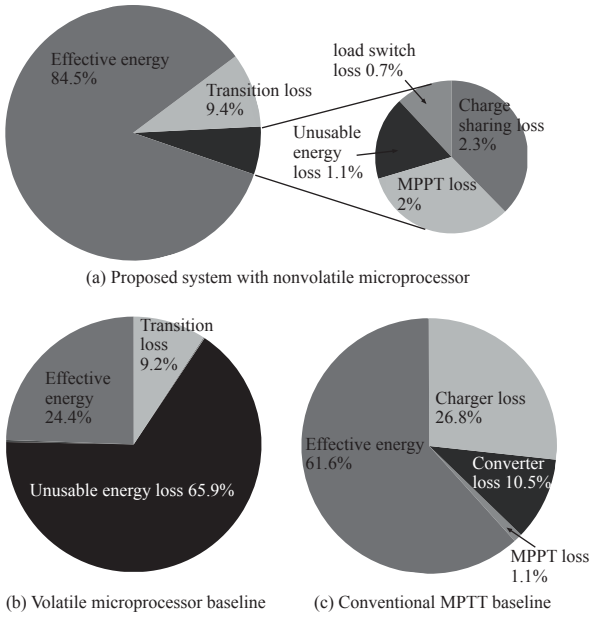

Fig. 7. Energy loss breakdown in the three different PV energy harvesting systems.

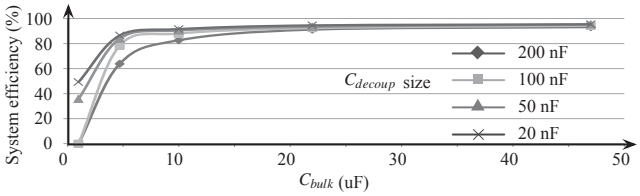

Fig. 8. Effects of the C_{bulk} and C_{decoup} on system efficiency.

Fig. 7 illustrates the energy loss breakdown, where effective energy represents the energy utilized for task execution. The proposed method incurs unusable energy loss because the PV output voltage is not high enough to reach the legal operating range of the system when solar irradiance is very weak. The proposed method is not equipped with an energy storage element nor a DC-DC converter, and should waste the harvested energy in such a case.

The proposed system loses 9.4% of the PV energy due to transition overheads while loses a total of 6.1% of the harvested energy due to charge sharing, MPP tracking, etc. The volatile microprocessor baseline does not work during a large proportion of the time due to the large transition overhead, resulting in a 65.9% "unusable energy loss". The energy loss due to state transitions is also considerable at around noon, accounting for 9.2% of the energy loss. Energy loss due to charge sharing and MPP tracking is 0.5% for the volatile microprocessor baseline, which is omitted in the pie graph. The conventional MPTT system loses most of energy in the two-stage converters, resulting an overall 61.6% of the energy utilized for task execution.

C. Effects of C_{bulk} and C_{decoup}

Fig. 8 shows the system efficiency over a wide range of C_{bulk} and C_{decoup} selection. The energy loss stemmed from charge sharing decreases as C_{decoup} shrinks, and the overall efficiency goes up. Fig. 9 shows how C_{bulk} affects the DPM period and energy loss. The DPM period, T_{dpm}, increases as the bulk capacitor becomes larger as shown in Fig. 9(a). This makes the state transition and charge sharing less

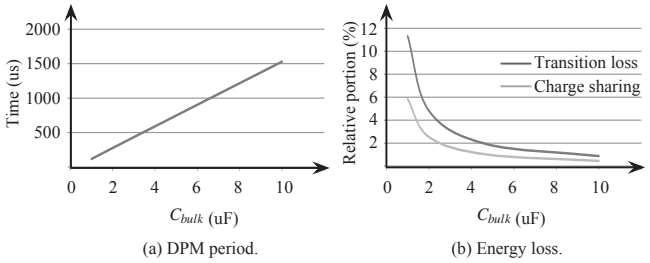

(a) DPM period. (b) Energy loss.

Fig. 9. Effects of the C_{bulk} on (a) DPM period and (b) Energy loss.

frequent, and therefore lower the energy loss due to them. This is also why the system efficiency improves as C_{bulk} increases, as observed in Fig. 8.

The overall efficiency of the proposed system reaches up to 95.4% if we enlarge the bulk capacitor to 47 μF. Enlarging the bulk capacitor size also improves the efficiency of the volatile microprocessor baseline. Nevertheless, the proposed system would still outperform the volatile microprocessor baseline because of its low transition overheads.

D. Prototype Board

We implement an evaluation prototype following Fig. 5(b) to validate the functionality and analysis of the proposed system. Fig. 10 is a photograph of the proposed storage-less and converter-less PV energy harvesting system with MPPT. The board contains a PV module, load switches, a nonvolatile microprocessor, an instruction memory, a clock module, measuring interfaces, testing interfaces, voltage regulators and an MSP430 micro-controller for the DPM control. The MSP430 is only used for development purpose. It is powered separately from an external power supply. A low-power CMOS circuit will replace MSP430 in the final design. The voltage regulators are also used for development purpose. They are bypassed in the proposed system. The instruction memory for the nonvolatile microprocessor is a one time programmable (OTP) ROM with a start-up time of 2 μs.

The PV cell output voltage and DPM control signal waveform captured from the evaluation prototype board are shown in Fig. 11, with $C_{bulk} = 47\mu F$, $C_{decoup} = 20nF$ and the nonvolatile microprocessor THU1010N running a counting program. The PV cell output voltage, depicted by the upper curve, swings within the MPP window of $[2.77\ V, 2.97\ V]$ under control of the DPM control signal.

VI. Conclusion

This paper introduces a breakthrough idea for maintenance-free long-lasting low-cost photovoltaic (PV) energy harvesting system. The proposed idea is a radical change of conventional design concept: use of the maximum power point tracking (MPPT) charger, an energy storage device, and a voltage regulator. These components are root causes of high cost, a short lifetime, large volume, and heavy weight. We eliminate the energy storage device and power converters (the charger and regulator) and directly connect the PV cell to the microprocessor. We perform MPPT through a very fine-grain dynamic power management of the nonvolatile microprocessor in every a few hundred microseconds. The efficiency benefit is significant. We achieve an overall system efficiency of 84.5%, and the proposed method makes the PV energy harvesting system operational even with a very weak solar irradiance. The benefits in terms of cost, volume and weight are even higher, and lifetime extension is not even comparable.

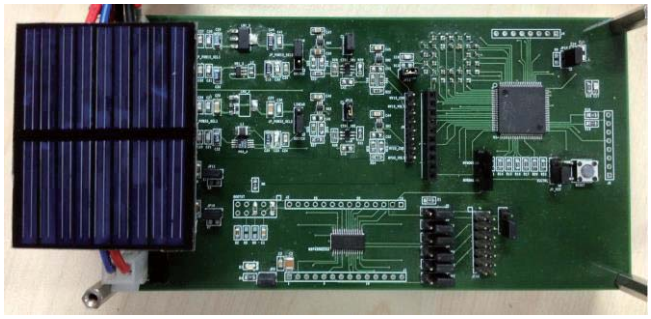

Fig. 10. Photograph of the prototype board for evaluation.

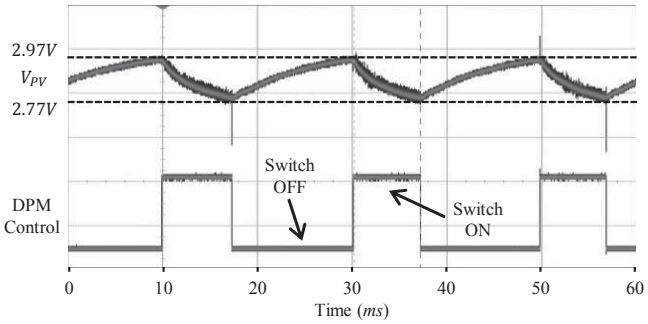

Fig. 11. Waveform of the evaluation prototype board in operation.

References

[1] T. Esram and P. Chapman, "Comparison of photovoltaic array maximum power point tracking techniques," *IEEE Trans. on Energy Conversion*, vol. 22, no. 2, pp. 439–449, 2007.

[2] Y. Kim, N. Chang, Y. Wang, and M. Pedram, "Maximum power transfer tracking for a photovoltaic-supercapacitor energy system," in *ISLPED*, 2010, pp. 307–312.

[3] N. Femia, G. Petrone, G. Spagnuolo, and M. Vitelli, "Optimization of perturb and observe maximum power point tracking method," *IEEE Trans. on Power Electronics*, vol. 20, no. 4, pp. 963–973, 2005.

[4] W. D. Soto, S. Klein, and W. Beckman, "Improvement and validation of a model for photovoltaic array performance," *Solar Energy*, vol. 80, pp. 78–88, January 2006.

[5] R. A. Messenger and J. Ventre, *Photovoltaic Systems Engineering, Third Edition*. CRC Press, 2010.

[6] D. Brunelli, C. Moser, L. Thiele, and L. Benini, "Design of a solar-harvesting circuit for batteryless embedded systems," *IEEE Trans. on Circuits and Systems I: Regular Papers*, vol. 56, pp. 2519–2528, 2009.

[7] F. Simjee and P. Chou, "Everlast: Long-life, supercapacitor-operated wireless sensor node," in *ISLPED*, 2006, pp. 197–202.

[8] Y. Choi, N. Chang, and T. Kim, "DC–DC converter-aware power management for low-power embedded systems," *IEEE Trans. on Computer-Aided Design of Integrated Circuits and Systems*, vol. 26, no. 8, pp. 1367–1381, 2007.

[9] Y. Liu, Y. Wang, H. Jia, S. Su, J. Wen, W. Zhang, L. Zhang, and H. Yang, "An energy harvesting nonvolatile sensor node and its application to distributed moving object detection," in *IPSN*, 2012, pp. 149–150.

[10] Y. Wang, Y. Liu, S. Li, D. Zhang, B. Zhao, M.-F. Chiang, Y. Yan, B. Sai, and H. Yang, "A 3us wake-up time nonvolatile processor based on ferroelectric flip-flops," in *Proceedings of the ESSCIRC*, 2012, pp. 149–152.